Evaluation of ECG Imaging to map haemodynamically stable and unstable ventricular arrhythmias

Running title: Simultaneous ECGI vs Contact mapping during VT

Adam J Graham MRCP[a]∗, Michele Orini PhD [a,b]∗, Ernesto Zacur PhD[c], Gurpreet Dhillon MRCP[a] , Holly Daw BSc[a], Neil T Srinivasan PhD MRCP[a], Claire Martin MRCP PhD[a], Jem Lane PhD MRCP[a], Josephine S Mansell MRCP[a], Alex Cambridge BSc[a], Jason Garcia BSc[a], Francesca Pugliese MD PhD[a], Oliver Segal MD MRCP[a], Syed Ahsan MD MRCP[a], Martin Lowe PhD FRCP[a], Malcolm Finlay PhD MRCP[a], Mark J Earley MD MRCP[a], Anthony Chow MD MRCP FHRS[a], Simon Sporton MD FRCP[a], Mehul Dhinoja MD MRCP FHRS[a], , Ross J Hunter MRCP FHRS PhD[a], Richard J Schilling MD MRCP FHRS[a], Pier D Lambiase PhD FRCP FHRS[ad]

a. Barts Heart Centre, Barts Health NHS Trust, West Smithfield, London EC1A 7BE, UK
b. Department of Mechanical Engineering, University College London, London, UK
c. Institute of Biomedical Engineering, University of Oxford, Oxford, UK.
d. Institute of Cardiovascular Science, University College London, Gower Street, London WC1E 6BT, UK

∗Equal contributors

Address for correspondence:
Professor Pier D. Lambiase
UCL Institute of Cardiovascular Science & Cardiology Dept, Barts Heart Centre, Barts Health NHS Trust, West Smithfield, London, EC1A 7BE, UK
Email: p.lambiase@ucl.ac.uk
Tel: 0203 765 8647

Key Words: Ventricular tachycardia, arrhythmia, catheter ablation, mapping , ECGI

Clinical Perspective

WHAT IS KNOWN?

- ECG imaging (ECGI) allows non-invasive reconstruction of epicardial unipolar electrograms using heart-torso geometry and body surface potentials in just 1 beat.
- The ECGI system has been recently introduced for clinical application, and it's accuracy has not been quantitatively assessed with simultaneous recordings during catheter ablation for ventricular tachycardia.

WHAT THE STUDY ADDS?

- ECGI outperforms the standard 12 lead surface ECG for localisation of VT circuits during VT ablation.
- The ECGI system localizes sites of origin of VT with a resolution of 22.6, 13.9—36.2 mm. A resolution that is insufficient to solely guide catheter ablation of VT but potentially sufficient for non-invasive radiation therapy.

Abstract

Background: ECG Imaging (ECGI) has been used to guide treatment of ventricular ectopy and arrhythmias. However, the accuracy of ECGI in localising the origin of arrhythmias during catheter ablation of ventricular tachycardia (VT) in structurally abnormal hearts remains to be fully validated.

Methods: During catheter ablation of VT, simultaneous mapping was performed using electro-anatomical mapping (EAM) (CARTO, Biosense-Webster) and ECGI (CardioInsight™, Medtronic) in 18 patients. Sites of entrainment, pace-mapping and termination during ablation were used to define the VT site of origin (SoO). Distance between SoO and the site of earliest activation on ECGI were measured using co-registered geometries from both systems. The accuracy of ECGI vs a 12-lead surface ECG algorithm was compared.

Results: A total of 29 VTs were available for comparison. Distance between SoO and sites of earliest activation in ECGI was 22.6, 13.9—36.2 mm (median, first—third quartile). ECGI mapped VT sites of origin onto the correct AHA segment with higher accuracy than a validated 12-lead ECG algorithm (83.3% vs 38.9%, P=0.015).

Conclusions: This simultaneous assessment demonstrates that CardioInsight™ localises VT circuits with sufficient accuracy to provide a region of interest for targeting mapping for ablation. Resolution is not sufficient to guide discrete radiofrequency lesion delivery via catheter ablation without concomitant use of an electro-anatomical mapping system, but may be sufficient for segmental ablation with radiotherapy.

Keywords: ECG imaging, ventricular tachycardia, catheter ablation, mapping, arrhythmia

Non-standard Abbreviations and Acronyms: Electroanatomical mapping, method of fundamental solutions (MFS), stereotactic body radiation therapy (SBRT), sites of origin (SoO), Activation time (AT).

Introduction

Clinical outcomes for catheter ablation of ventricular tachycardia (VT) remain sub-optimal despite advances in mapping technology[1]. Mapping is frequently limited by haemodynamic instability, hence substrate based ablation strategies have been developed to combat this with varied results due to lack of consensus in the criteria for targeting pro-arrhythmic sites and limitations of lesion delivery [2]. The ability to accurately and expediently map exit sites in unstable VT could offer promise to improve outcomes and the efficiency of procedures [3]. Electrocardiographic imaging (ECGI) employs body surface electrodes combined with a patient specific CT or MRI derived epicardial geometry to display the full sequence of electrical activity during a single beat over the whole heart hence providing a panoramic map of the arrhythmia [4]. This is achieved using an inverse method described and tested in prior publications [5–7] and commercial ECGI systems, e.g. CardioInsight™, have recently become available for clinical applications. This commercial system uses the method of fundamental solutions (MFS) to solve the inverse problem of electrocardiography. Other methods have been developed, attempting to correct for inhomogeneities between the epicardial surface and body surface, with as yet no improvement in accuracy [8].

Clinically, ECGI has been utilised in ablation of ventricular ectopy [9,10] and a non-commercial research-oriented ECGI system has been used most recently to direct stereotactic body radiation therapy (SBRT), in failed radiofrequency ablation VT cases [11,12]. However, there has been limited study of arrhythmias in structural heart disease and limited simultaneous validation during VT [13]. Following an initial study focusing on simultaneous comparison of ECGI derived versus contact-mapping measured unipolar electrogram and activation/repolarization maps [14], we studied the accuracy

of the commercially available ECGI system CardioInsight™ in mapping haemodynamically stable and unstable VT using contact electro-anatomical mapping (EAM) data collected simultaneously as a reference.

Methods

Because of the sensitive nature of the data collected for this study, requests to access the dataset from qualified researchers trained in human subject confidentiality protocols may be sent to Professor Pier Lambiase, UCL, London at p.lambiase@ucl.ac.uk.

The study was approved by the National Research Service Committee, London (14/LO/0360). Thirty-seven patients undergoing catheter ablation of VT were recruited for the study. Ten of these were elective, with the remaining being emergency procedures. All patients were scheduled for a catheter ablation on clinical grounds for structurally abnormal heart VT and gave their informed consent to participate in the research study.

Clinical Method

Procedures were performed under conscious sedation using Diamorphine and Midazolam or general anaesthetic. Endocardial access was obtained under ultrasound guidance using Seldinger technique via the right femoral vein +/- right femoral artery. All patients were planned for endocardial access to the right ventricle (RV) +/- left ventricle (LV) access via trans-septal puncture or retrogradely via the aorta. A sub-

xiphisternal puncture using a Tuohy needle, with fluoroscopic guidance, was used to access the epicardial space in five patients, using a previously described technique [15].

A full geometry of the ascending, arch and descending aorta was created for co-registration with ECGI (Figure 1A). If arterial access was not part of the procedure, detailed geometry from either the right ventricular outflow tract (RVOT) and the inferior and superior vena cava (IVC and SVC), or the left atrium (LA) (if trans-septal puncture) was collected (Figure 1B).

Ventricular tachycardia was induced with a standard Wellens protocol from the RV apex. If no VT was induced the protocol was repeated from the RVOT or LV. An EAM (CARTO, Biosense-Webster, CA, USA) was created during VT using a multipolar catheter or by point-by-point mapping (Pentarray, Decapolar or SmarTouch, Biosense-Webster, CA, USA). In haemodynamically tolerated VTs identification of sites of origin (SoO) was defined by entrainment or termination with ablation. Entrainment at a cycle length 20 ms shorter than the VT was attempted at sites where diastolic activity was seen. For the purpose of the study a rhythm was considered entrained when concealed fusion with a post-pacing interval (PPI) minus tachycardia cycle length of <30 ms was present and the S-QRS was <50% of the tachycardia cycle length[16]. In the case of unstable VT or non-sustained VT, pace-mapping was performed and the average correlation coefficient between the 12 lead ECG of VT and the paced beat was calculated using the Bard EP system (Boston Scientific, MA, USA). An average correlation coefficient ≥90% was taken as a surrogate marker of the VT SoO/exit zone [17]. The location on the EAM of these sites was recorded.

ECGI

Prior to catheter ablation, a 252-electrode vest (CardioInsight™, Medtronic, MN, USA) was fitted for recording of body surface potentials (sampling rate 1000 Hz) and remained in situ until conclusion of the procedure. A non-contrast axial CT scan with 3 mm slice thickness was performed up to four hours before the procedure. Patient-specific epicardial geometry was created using the EcVue system (Medtronic, MN, USA) with data from the CT and body surface potentials. Epicardial unipolar electrograms were computed over approximately 1400 epicardial points covering both ventricles using torso-heart geometry and unfiltered body surface potentials. Reconstructed unipolar electrograms over the atrioventricular valves were excluded from the analysis. Activation time (AT) and voltage maps were created for all induced VTs.

Co-registration of EAM and ECGI geometries was performed semi-automatically with bespoke software (Matlab, The Mathworks Inc., MA, USA) as in our previous study [14]. Figure 1 shows alignment of ECGI and EAM geometries including the Aorta, LA and IVC and RVOT. The optimal co-registration was visually determined by two experts independent of subsequent analysis.

The VT SoO was projected from the co-registered EAM onto the nearest node of the ECGI geometry, including for SoO localised to the septum.

Unipolar electrograms from ECGI were analysed blindly to VT SoO (Matlab, The Mathworks Inc., MA, USA). Signals were band-pass filtered between 0.5 and 80 Hz and activation time (AT) was measured as the time of the steepest signal downslope (dV/dt_{min}) during the QRS complex [18,19]. In ECGI multiple sites may share the same AT. Therefore, the site of earliest activation was defined as the nearest site to the centre of the region of earliest activation (area including 2% of sites showing earliest

activation). The closest site to the centre of the area of earliest negative voltage was also utilized to localize earliest sties of activation [20]. This was defined as the area including the first 2% of sites showing a voltage lower than a patient-specific noise threshold (1/3 of the absolute minimum potential).

The Euclidean distance between the VT SoO and the earliest activation sites on ECGI was calculated to assess ECGI spatial resolution for VT mapping.

All signals and markers were carefully reviewed and semi-automatically corrected if needed as in previous studies[21,22].

12 Lead ECG Comparison

Twelve lead body surface ECGs were recorded throughout the cases using Bard EP system (Boston Scientific, MA, USA) with filters set between 0.5-100 Hz. A contemporary algorithm that allocates the VT SoO to one of the 17 myocardial segments of the standard AHA model was implemented[23]. The ECGs for each mapped VT were analysed by 2 experts who allocated the SoO onto the corresponding cardiac segment by following the algorithm. A third electrophysiologist arbitrated any discrepancies. Both were blinded to results of EAM and ECGI maps. ECGI and EAM were allocated a segment based on the position of the earliest site of activation and the SoO, on ECGI and EAM respectively, with the central point in the region of earliest activation used for ECGI. Given ECGI reconstructs epicardial potentials only, VTs with a septal SoO on the EAM were excluded from the 17-segment model comparison portion of the analysis. SoO from the RV were also excluded as they are not part of the AHA 17 segment model.

Statistical analysis

Data distribution is described by median, first-third quartiles. Statistical differences were assessed using the Wilcoxon rank sum test for unpaired comparisons and the Wilcoxon signed rank test for paired comparisons. Differences between the proportion of correct cardiac segments identified by ECGI or 12-Lead ECG were assessed using the exact Fisher's test. Threshold for statistical significance was 0.05. Statistical analysis was performed in Matlab, MathWorks.

Results

Nineteen of the 37 patients prospectively recruited were excluded from the final analysis. Five were non-inducible (26.3%), 3 due to procedural complications (15.8%), 1 due to ECGI equipment failure (5.3%) and 10 on account of haemodynamically non-tolerated VT with no suitable pace-mapping (52.6%). Absence of pace-mapping was on account of inability to pace from areas producing adequate morphology match or due to termination of case before pace-mapping was employed. Procedural complications were unrelated to ECGI. One patient had a groin complication, 1 a large pericardial effusion during epicardial access and 1 became hypotensive during the procedure.

Eighteen patients were studied, of which 4 had Dilated Cardiomyopathy DCM (22.2%), 4 Arrhythmogenic RV Cardiomyopathy (22.2%) and 10 ischaemic heart disease (IHD) (55.6%) (Table 1). 29 different VT circuits mapped using EAM of which 20 (69%) where haemodynamically stable and 9 (31%) unstable. Epicardial access was utilised in 5 patients (27.8%). Three VTs were mapped to the epicardium (10%) and 26 (90%) to the endocardium. Of the endocardial VTs, 6 were localised to the septum (5 LV and

1 RV) and 6 the RV. The remaining were mapped to the LV anterior, inferior or lateral walls. The SoO was located with entrainment in 11 VTs (38%), termination with ablation in 9 VTs (31%) and pace mapping in 9 VTs (31%). If a rhythm was entrained and then subsequently terminated with ablation, for the purpose of analysis this was recorded as entrained (Table 2).

ECGI localisation of VT Circuits

Co-registration of ECGI and EAM geometries utilised the Aorta in 11 patients (61.1%), LA in 4 patients (22.2%) and IVC and RVOT in 3 patients (16.7%).

Of the 11 entrained VTs, 9 (81.9%) presented lines of block adjacent to the region of earliest activation (Supplementary Figure 1). In general however, the VT circuit, which could involve intramural pathways, was not discernible from ECGI AT maps. In the region of earliest activation, the ECGI unipolar electrograms showed a QS complex typical of earliest activation independent of endocardial as opposed to epicardial origin (Supplementary Figure 2).

Figures 2, 3 and 4 show examples of VTs terminated with ablation, pace-mapped, and entrained, respectively.

The distance between the site of earliest activation on ECGI and the nearest ECGI point to the VT SoO registered on EAM was 22.6, 13.9–36.2 mm (median, 1st-3rd quartile) (Table 2). This was not significantly different between VTs that were pace-mapped, entrained or terminated with ablation ($P>0.3$), or between VTs mapped on the RV vs LV ($P=0.47$), while borderline non-significant differences existed between ischaemic (26.6, 18.5-39.1 mm) and non-ischaemic patients (15.8, 9.6-21.6 mm), $P=0.055$. In 7 patients, more than 1 VT was mapped, with an average distance per patient of 18.2, 14.8-34.7 mm. In two of the 3 VTs mapped onto the epicardium, distance from earliest site of activation in ECGI and VT SoO was lower than the

median (14.2 and 17.3 mm), whereas in the remaining case the distance was much larger as in this case ECGI showed 2 distinct regions of earliest activation, with the earliest being located on the opposite site of the heart.

Using time to earliest negative voltage instead of AT to define the earliest site of activation provided significantly lower resolution, with distance from VT SoO equal to 34.6, 18.8-45.4 mm (P=0.039).

Supplementary Table 1 shows results of further analysis, including distance from the site of earliest activation in ECGI to the original VT SoO registered on the EAM (without projecting it onto the nearest ECGI point) of 26.1, 13.9-36.2 mm and distance from the VT SoO to the margin of the area of earliest activation (surface 3.4, 1.8-4.3 cm^2) of 13.0, 3.4-24.0 mm.

ECGI localised the SoO of the VT to the correct anatomical AHA segment in 15 out of 18 cases (83.3%) whereas the 12-lead algorithm identified the correct anatomical segments in 7 out of 18 cases (38.9%), P=0.015 (see Table 2).

Discussion

This is the first simultaneous assessment of an ECGI approach to localise VT sites of origin during catheter ablation in structurally abnormal hearts. Due to its spatial resolution, EAM provides a suitable reference for ECGI assessment[24]. We have demonstrated that CardioInsight™ localizes VT sites of origin with a spatial resolution of 22.6, 13.9–36.2 mm (median, first-third quartile). ECGI localised VT SoO to the correct AHA anatomical segment in 83.3% of VTs studied, outperforming a recently proposed 12 lead ECG algorithm[23].

A recent study has questioned the accuracy of CardioInsight™ activation time maps, including the localization of epicardial breakthrough, during sinus rhythm [25]. Given the marked differences in conduction dynamics between sinus rhythm and re-entrant ventricular tachycardia as well as different methodological analysis, our results cannot be directly compared. One may however speculate that the resolution required to correctly localise the VT SoO may be lower than the resolution required to track the activation sequence when the normal conduction system is engaged.

Previous studies have examined the capacity of ECGI to localise paced beats [6,26–31]. In experimental studies using tank-torso models, the accuracy has been shown to be <10 mm [30,31]. Similar accuracy was seen in humans when localising RV endocardial and LV epicardial pacing from the coronary sinus [5]. Given ECGI reconstructs epicardial potentials, accuracy should be superior with direct pacing on the epicardium, when compared to endocardial pacing. However, a human study using an ECGI system based on 120-lead body-surface potential mapping reported distances to the SoO of 13.5±9 mm and a recent study from our group showed similar results [14]. In a similar study in canines using direct contact epicardial electrodes accuracy was 10 mm [27]. Although this latter study utilised a different inverse method, therefore comparison could be limited. Bear et al. (2018) in a porcine model utilised a similar inverse method to the one employed in our study and found an accuracy of 16 mm for localising epicardial foci [32].

The localisation of pacing sites provides a surrogate marker for arrhythmia localisation [4]. Two studies have examined the role of ECGI in mapping ventricular ectopy (VE). ECGI showed superior capability to localise VE origins when compared to 12 lead algorithms and facilitated faster times to ablation[9,10]. For sustained VT, accurate

reconstruction of activation sequences has been demonstrated in heart torso-tank models using canine hearts, where average accuracy of localisation was 8.69 mm [33]. In humans, ECGI was accurate in a heterogeneous group of patients with both normal and abnormal hearts, and mainly focal VT[13]. Comparison between contact mapping and ECGI in both the VE [9,10] and VT[13] studies was based on location of an anatomical segment of the heart and not a distance to the point of earliest activation. In contrast, our data contains only structurally abnormal heart VT, with induced VTs most likely to be re-entrant in mechanism. Given the re-entrant mechanism, distance from SoO to early activation on ECGI, could have been expected to be shorter for pace-mapped than entrained or terminated with ablation VTs. This was not the case in this study.

The ability to expeditiously differentiate between focal and re-entrant VTs could influence subsequent contact mapping and ablation strategy. ECGI has been shown previously to differentiate between these[13]. We found 81.8% of entrained VTs were suggestive of a macro re-entrant mechanism on ECGI, with lines of block seen in areas adjacent to areas of early activation. Although the limited number included in this study precludes definitive conclusions being drawn, in this study ECGI did not accurately reconstruct re-entrant sequences for all VTs of this type. Figure 2 illustrates an example of accurate localisation of SoO on ECGI for a re-entrant VT. The projected point from the SoO on the EAM can be seen within the area of earliest activation on ECGI. However, the direction of the propagation through the diastolic pathway on the EAM, and bipolar electrograms recorded from the decapolar catheter, would suggest activation is occurring from high to low. The ECGI map suggests the converse of this. The reasoning for this is uncertain and could represent an artefactual line of block, as has been reported by other investigators[25,34].

ECGI is also purported to differentiate between epicardial and endocardial VT's[13,28,31], as epicardial unipolar electrograms should exhibit an rS wave for endocardial and a pure Q wave for epicardial sites of origin. Despite being unable to directly compare accuracy of epicardial vs endocardial VTs due to insufficient data points, our findings do not support the use of ECGI to accomplish this. None of the VTs localised to the endocardium on EAM showed evidence of rS complexes in the region of early activation (see supplementary figure 2). If an endocardial site of earliest activation arising from a region of dense scar conducts epicardially then this could explain why only Q waves are seen in a region of earliest activation on ECGI, as there is insufficient tissue to generate the electromotive force to form an R wave, hence only the epicardial breakthrough is identified as a Q wave in more superficial viable tissue. This casts doubt on ECGI being able to discern whether epicardial access is warranted based on the reconstructed electrograms from VT beats in structural heart disease.

The localization of VTs with septal origin would be expected to be less accurate as only epicardial electrograms are reconstructed. However, our data indicates that accuracy of the location of septal VTs was similar to those located elsewhere in the heart. Further data and clinical algorithm development are required to determine if ECGI can provide information on the depth of the SoO on the septum or indeed if further processing of the unipolar signals is needed to improve the identification of endo, mid- or epicardial origins. Furthermore, we found no difference in the localisation of RV and LV VTs. This is in spite of the differing wall thickness between the ventricles.

Our data demonstrated an accuracy of 83.3% with ECGI when the 17-segment model was used, which compares to over 90% accuracy in localising mostly focal VT shown

in a previous ECGI study [13]. The 12 lead ECG algorithm used for comparison in this study has been validated previously examining the 17 segment model in structural heart disease showing 81.9% of VTs localised in ischaemic and non-ischaemic cardiomyopathy with equivalent accuracy in non-septal VTs (83%) [23]. Its applicability to various forms of heart disease was the rationale for our use of this particular algorithm. By providing more accurate localisation of VT SoO than the 12 lead ECG, ECGI could better guide targeted ablation, particularly in haemodynamically unstable VT. The increased accuracy of ECGI in comparison to the 12 lead ECG could be a feature of ECGI taking into account individual heart-torso geometry and rotation, and the use of multiple body surface electrodes providing more electrical data.

This study has highlighted a number of features that could be developed to optimise the system including refinement of signal processing and algorithms for allocation of activation times to reconstructed electrograms. Indeed, additional work will be required to isolate diastolic potentials during VT if this is possible. Furthermore, integration of ECGI epicardial maps into a common geometry within an EAM system to enable targeted ablation will be a major advance. Treatment of VT using stereotactic body radiation therapy (SBRT), guided in part by ECGI localisation of VT, has shown promising results as VT episodes decreased from 119 (4-292) to 3 (0-31) at 6 months post treatment [11,12]. A single segment of VT origin was targeted with a more homogenous lesion delivery versus conventional radio-frequency ablation. This novel methodology has thus far been performed in a single centre and further research will be needed into both its long-term efficacy and the role played by ECGI. At present the precision of ECGI may be sufficient to enable application of this form of energy without the need for additional mapping as the area of lesion delivery is larger: 17-81 ml versus

401 “point by point” radiofrequency ablation coupled with the more homogeneous tissue
402 effects. Furthermore, ECGI localises the VT exit site as opposed to the diastolic
403 pathway as we are unable to discern diastolic potentials, even in the epicardial VT
404 cases. The exit site will co-localise adjacent to the diastolic pathway in the majority of
405 cases which can be compensated for by a wider area of ablation of radiation energy
406 and will also be more transmural. However, mapping of the diastolic pathway with
407 EAM will still be required if more localised radiofrequency energy is to be delivered to
408 the critical component of the circuit.
409

410 ***Limitations***

411 There are inherent limitations posed by EAM and pacing manoeuvres to locate VT
412 SoO. Pace-mapping accuracy can be affected by area of capture and functional block
413 only present in VT[16]. Pace mapping was performed at the lowest outputs to ensure
414 consistent myocardial capture but was not performed at the VT cycle length [17]. A
415 previous study has reported 82% sensitivity and 87% specificity in identifying the exit
416 region by pace mapping with a 82% morphology match [17] . Our choice of using a cut
417 off value of 90% morphology match to identify SoO is expected to provide slightly
418 higher specificity, with a spatial resolution which needs to be assessed in future
419 studies. Furthermore, given that ECGI reconstructs unipolar epicardial electrograms
420 our methodology of locating SoO, mainly on the endocardium, represents an indirect
421 comparison and introduces potential error. Points of entrainment with S-QRS interval
422 between 30-50% of the tachycardia cycle length can be remote from the exit site. The
423 inclusion of these points may have resulted in an overestimation of the distance
424 between the VT exit site and the point of earliest activation on ECGI[35].
425

Accuracy of the ECGI maps could have been affected by alterations in the relationship between the heart and torso during the cardiac and respiratory cycle[36]. To our knowledge no adequate correction for this is currently available. Despite using fixed anatomical landmarks, the co-registration of the geometries could still introduce error. Visually the aorta is the easiest anatomical structure to co-register and for future research, and potential clinical application, may offer the best means of effective alignment of geometries from different systems. Movements of up to 4 mm and rotations of up to 5° have been previously shown to alter correlation co-efficient between activation time maps on EAM and ECGI by up to 25%[14]. An integrated ECGI and EAM system with electrogram data presented in a common geometry would overcome this issue. Finally, reported Euclidean distances could be smaller than distances accounting for the curved surface of the heart, and the statistical analysis is limited by the small number of VTs included.

Conclusion

ECGI provides sufficient resolution to identify myocardial segments with sites of earliest activation in VT, but in its current iteration would be insufficient to guide catheter ablation without detailed contact mapping. However, it may be sufficient for targeting radiotherapy-based strategies or energies that deliver transmurally over a wider area than current discrete radiofrequency lesion sets. The capacity to give a region of interest could facilitate efficient targeted mapping and ablation of haemodynamically unstable VTs out-performing the 12 lead ECG.

Funding Sources

Dr Adam Graham is supported by Barts Charity

Dr Michele Orini is supported by British Heart Foundation grant PG/16/81/32441

Prof P. Lambiase is supported by UCLH Biomedicine NIHR and Barts BRC.

The study was in part supported by a Medtronic External Research Program grant.

Disclosures

Professor Pier Lambiase receives educational grants and speaker fees from Medtronic. All other authors have nothing to disclose.

References

1. Josephson ME, Anter E. Substrate Mapping for Ventricular Tachycardia Assumptions and Misconceptions. JACC Clin. Electrophysiol. 2015;1:341–352.
2. Santangeli P, Marchlinski FE. Substrate mapping for unstable ventricular tachycardia. *Heart Rhythm*. 2016;13:569–583.
3. Dubois R, Shah AJ, Hocini M, Denis A, Derval N, Cochet H, Sacher F, Bear L, Duchateau J, Jais P, Haissaguerre M. Non-invasive cardiac mapping in clinical practice: Application to the ablation of cardiac arrhythmias. Journal of Electrocardiology. 2015. 48(6):966-74
4. Rudy Y, Lindsay BD. Electrocardiographic imaging of heart rhythm disorders. From bench to bedside. Card. Electrophysiol. Clin. 2015;7:17–35.
5. Wang Y, Rudy Y. Application of the method of fundamental solutions to potential-based inverse electrocardiography. *Ann Biomed Eng*. 2006; 34(8): 1272–1288.
6. Oster HS, Taccardi B, Lux RL, Ershler PR, Rudy Y. Electrocardiographic imaging: noninvasive characterization of intramural myocardial activation from inverse-reconstructed epicardial potentials and electrograms. *Circulation*. 1998;97:1496–1507.
7. Burnes JE, Taccardi B, Rudy Y. A noninvasive imaging modality for cardiac arrhythmias. *Circulation*. 2000;102:2152–2158.
8. Cluitmans M, Brooks DH, MacLeod R, Dössel O, Guillem MS, Van Dam PM, Svehlikova J, He B, Sapp J, Wang L, et al. Validation and opportunities of electrocardiographic imaging: From technical achievements to clinical applications. Front. Physiol. 2018; 20;9:1305
9. Jamil-Copley S, Bokan R, Kojodjojo P, Qureshi N, Koa-Wing M, Hayat S, Kyriacou A, Sandler B, Sohaib A, Wright I, et al. Noninvasive electrocardiographic mapping to guide ablation of outflow tract ventricular arrhythmias. *Heart Rhythm*. 2014;11:587–594.
10. Erkapic D, Greiss H, Pajitnev D, Zaltsberg S, Deubner N, Berkowitsch A, Möllman S, Sperzel J, Rolf A, Schmitt J, et al. Clinical impact of a novel three-dimensional electrocardiographic imaging for non-invasive mapping of ventricular arrhythmias - A prospective randomized trial. *Europace*.

2015;17:591–597.
11. Robinson CG, Hugo GD, Lang A. Phase I/II Trial of Electrophysiology-Guided Noninvasive Cardiac Radioablation for Ventricular Tachycardia. Circulation. 2019;139:313–321
12. Cuculich PS, Schill MR, Kashani R, Mutic S, Lang A, Cooper D, Faddis M, Gleva M, Noheria A, Smith TW, et al. Noninvasive Cardiac Radiation for Ablation of Ventricular Tachycardia. *N Engl J Med*. 2017;377:2325–2336.
13. Wang Y, Cuculich PS, Zhang J, Desouza KA, Vijayakumar R, Chen J, Faddis MN, Lindsay BD, Smith TW, Rudy Y. Noninvasive Electroanatomic Mapping of Human Ventricular Arrhythmias with Electrocardiographic Imaging. *Sci Transl Med*. 2011;3: 98ra84
14. Graham AJ, Orini M, Zacur E, Dhillon G, Daw H, Srinivasan NT, Lane JD, Cambridge A, Garcia J, O'Reilly NJ, et al. Simultaneous Comparison of Electrocardiographic Imaging and Epicardial Contact Mapping in Structural Heart Disease. *Circ Arrhythm Electrophysiol*. 2019;12:e007120.
15. Sosa E, Scanavacca M, D'Avila A, Pilleggi F. A new technique to perform epicardial mapping in the electrophysiology laboratory. *J Cardiovasc Electrophysiol*. 1996;7:531–536.
16. Tung R, Mathuria N, Michowitz Y, Yu R, Buch E, Bradfield J, Mandapati R, Wiener I, Boyle N, Shivkumar K. Functional pace-mapping responses for identification of targets for catheter ablation of scar-mediated ventricular tachycardia. *Circ Arrhythmia Electrophysiol*. 2012;5:264–272.
17. De Chillou C, Groben L, Magnin-Poull I, Andronache M, Abbas MM, Zhang N, Abdelaal A, Ammar S, Sellal JM, Schwartz J, et al. Localizing the critical isthmus of postinfarct ventricular tachycardia: The value of pace-mapping during sinus rhythm. *Heart Rhythm*. 2014; 11(2):175-81.
18. Coronel R, de Bakker JMT, Wilms-Schopman FJG, Opthof T, Linnenbank AC, Belterman CN, Janse MJ. Monophasic action potentials and activation recovery intervals as measures of ventricular action potential duration: Experimental evidence to resolve some controversies. *Heart Rhythm*. 2006; 3(9):1043-50
19. Orini M, Taggart P, Lambiase PD. In vivo human sock-mapping validation of a simple model that explains unipolar electrogram morphology in relation to

conduction-repolarization dynamics. *J Cardiovasc Electrophysiol*. 2018; 29(7):990-997

20. Rudy Y, Burnes JE. Noninvasive electrocardiographic imaging. *Ann Noninvasive Electrocardiol*. 1999;4:340–359.
21. Orini M, Taggart P, Srinivasan N, Hayward M, Lambiase PD. Interactions between activation and repolarization restitution properties in the intact human heart: In-vivo whole-heart data and mathematical description. *PLoS One*. 2016; 11(9):e0161765
22. Martin CA, Orini M, Srinivasan NT, Bhar-Amato J, Honarbakhsh S, Chow AW, Lowe MD, Ben-Simon R, Elliott PM, Taggart P, et al. Assessment of a conduction-repolarisation metric to predict Arrhythmogenesis in right ventricular disorders. *Int J Cardiol*. 2018; 15;271:75-80
23. Andreu D, Fernández-Armenta J, Acosta J, Penela D, Jáuregui B, Soto-Iglesias D, Syrovnev V, Arbelo E, Tolosana JM, Berruezo A. A QRS axis–based algorithm to identify the origin of scar-related ventricular tachycardia in the 17-segment American Heart Association model. *Heart Rhythm*. 2018; 15(10):1491-1497
24. Gepstein L, Hayam G, Ben-Haim SA. A novel method for nonfluoroscopic catheter-based electroanatomical mapping of the heart: In vitro and in vivo accuracy results. *Circulation*. 1997;95:1611–1622.
25. Duchateau J, Sacher F, Pambrun T, Derval N, Chamorro-Servent J, Denis A, Ploux S, Hocini M, Jaïs P, Bernus O, et al, Dubois R. Performance and limitations of noninvasive cardiac activation mapping. *Heart Rhythm*. 2019;16:435–442.
26. Sapp JL, Dawoud F, Clements JC, Horáček BM. Inverse solution mapping of epicardial potentials: Quantitative comparison with epicardial contact mapping. *Circ Arrhythmia Electrophysiol*. 2012;5:1001–1009.
27. Cluitmans MJM, Bonizzi P, Karel JMH, Das M, Kietselaer BLJH, de Jong MMJ, Prinzen FW, Peeters RLM, Westra RL, Volders PGA. In Vivo Validation of Electrocardiographic Imaging. *JACC Clin Electrophysiol*. 2017;3:232–242.
28. Ghanem RN, Jia P, Ramanathan C, Ryu K, Markowitz A, Rudy Y. Noninvasive electrocardiographic imaging (ECGI): comparison to intraoperative mapping in patients. *Heart Rhythm*. 2005; 2(4):339-54

29. Revishvili AS, Wissner E, Lebedev DS, Lemes C, Deiss S, Metzner A, Kalinin V V., Sopov O V., Labartkava EZ, Kalinin A V, et al. Validation of the mapping accuracy of a novel non-invasive epicardial and endocardial electrophysiology system. *Europace*. 2015; 17(8): 1282–1288

30. Ramanathan C, Jia P, Ghanem R, Calvetti D, Rudy Y. Noninvasive electrocardiographic imaging (ECGI): Application of the generalized minimal residual (GMRes) method. *Ann Biomed Eng*. 2003; 31(8): 981–994

31. Oster HS, Taccardi B, Lux RL, Ershler PR, Rudy Y. Noninvasive electrocardiographic imaging: Reconstruction of epicardial potentials, electrograms, and isochrones and localization of single and multiple electrocardiac events. *Circulation*. 1997;96:1012–1024.

32. Bear LR, LeGrice IJ, Sands GB, Lever NA, Loiselle DS, Paterson DJ, Cheng LK, Smaill BH. How Accurate Is Inverse Electrocardiographic Mapping? *Circ Arrhythmia Electrophysiol*. 2018; 11(5):e006108

33. Burnes JE, Taccardi B, Ershler PR, Rudy Y. Noninvasive electrocardiographic imaging of substrate and intramural ventricular tachycardia in infarcted hearts. *J Am Coll Cardiol*. 2001;38:2071–2078.

34. Bear LR, Huntjens PR, Walton RD, Bernus O, Coronel R, Dubois R. Cardiac electrical dyssynchrony is accurately detected by noninvasive electrocardiographic imaging. *Heart Rhythm*. 2018; 5(7):1058-1069

35. Stevenson WG, Khan H, Sager P, Saxon LA, Middlekauff HR, Natterson PD, Wiener I. Identification of reentry circuit sites during catheter mapping and radiofrequency ablation of ventricular tachycardia late after myocardial infarction. *Circulation*. 1993; 88:1647–1670.

36. Cluitmans MJM, Peeters RLM, Westra RL, Volders PGA. Noninvasive reconstruction of cardiac electrical activity: Update on current methods, applications and challenges. Netherlands Hear. J. 2015; 23(6):301-11

Tables

Table 1: Baseline Characteristics for patients included in analysis. M: Male, F: female, IHD: Ischaemic heart disease, DCM: Dilated Cardiomyopathy, ARVC: arrhythmogenic right ventricular cardiomyopathy, Ao: Aorta, RV: right ventricular, RVOT: right ventricular outflow tract, SVC: superior vena cava, IVC: inferior vena cava, LA: Left Atria.

Patient	Age	Sex	Aetiology	ICD	LVEF	Anti-Arrhythmics	Anatomical Structure
1	73	M	IHD	Y	20	Bisoprolol, Amiodarone	Ao
2	22	M	ARVC	N	>55	Bisoprolol	RVOT, SVC, IVC
3	43	M	ARVC	Y	>55	Sotalol	Ao
4	54	M	DCM	Y	>55	Bisoprolol, Amiodarone	Ao
5	81	M	IHD	Y	25	Bisoprolol, Amiodarone, Mexiltine	Ao
6	82	M	IHD	Y	22	Bisoprolol, Amiodarone	LA
7	76	F	IHD	Y	20	Bisoprolol, Amiodarone	Ao
8	24	F	ARVC	N	>55	Flecainide	RVOT, SVC, IVC
9	79	M	IHD	Y	30	Bisoprolol, Amiodarone, Mexiltine	Ao
10	78	M	IHD	Y	15	Bisoprolol, Amiodarone	Ao
11	55	M	DCM	Y	45	Sotalol	LA
12	78	M	IHD	Y	14	Bisoprolol	Ao
13	69	M	IHD	Y	10	Bisoprolol, Amiodarone	Ao
14	79	M	IHD	Y	25	Bisoprolol, Mexilitine	LA
15	82	M	DCM	Y	45	Bisoprolol, Amiodarone	LA
16	52	F	ARVC	Y	>55	Sotalol	RVOT, SVC, IVC
17	22	M	DCM	Y	40	Bisoprolol, Amiodarone	Ao
18	84	M	IHD	Y	20	Bisoprolol, Mexilitine, Amiodarone	Ao

Table 2: Localisation of VT sites of origin (SoO) using ECGI. Site of origin was determined by pace-mapping (PM), entrainment (ENTR) or termination with ablation (ABL). Distance to VT SoO: Distance from the site of earliest activation on ECGI to the VT SoO registered on the EAM. Indication of whether the correct anatomical segment of the VT SoO was identified by ECGI or by a 12-lead ECG algorithm is given by ✓: Match. ×: No Match. N/A: Not available (RV and septal VTs were excluded as not represented either in AHA or ECGI).

VT	Pts	Localisation of VT SoO	ENTR	ABL	PM	Distance to VT SoO (mm)	AHA Segm. ECGI	AHA Segm. 12-L ECG
1	1	LV Basal Anteroseptal			✓	25.4	N/A	N/A
2	1	LV Basal Anterior			✓	37.5	✓	✓
3	2	RV Inferior			✓	19.7	N/A	N/A
4	3	RV Lateral Wall	✓			13.3	N/A	N/A
5	4	RVOT	✓			35.8	N/A	N/A
6	5	LV Basal Inferolateral	✓			35.1	✓	×
7	5	LV Basal Inferior	✓			39.4	✓	×
8	5	LV Basal Anterior		✓		67.1	×	✓
9	5	LV Mid inferolateral		✓		23.6	✓	×
10	5	LV Basal Inferolateral	✓			39.0	✓	×
11	6	LV Mid inferolateral		✓		39.5	×	✓
12	7	LV Mid anteroseptal		✓		54.5	N/A	N/A
13	8	LV Mid anterior (EPI)		✓		14.2	✓	✓
14	8	RVOT	✓			7.4	N/A	N/A
15	9	LV Mid inferolateral		✓		4.1	✓	×
16	9	LV Basal inferolateral	✓			25.1	✓	×
17	10	LV Mid anterior	✓			32.3	×	×
18	10	LV Mid anterolateral		✓		26.6	✓	×
19	11	RV Septum	✓			3.4	N/A	N/A
20	11	LV Basal Anteroseptal	✓			10.7	N/A	N/A
21	11	LV Basal Anteroseptal	✓			20.6	N/A	N/A
22	12	LV Mid inferolateral			✓	17.0	✓	×
23	13	LV Mid anterior			✓	6.9	✓	✓
24	14	LV Mid anteroseptal			✓	14.1	N/A	N/A
25	15	LV Basal Anterior		✓		22.6	✓	×
26	15	LV Basal Anterior			✓	8.5	✓	✓
27	16	LV RV Free wall (EPI)			✓	76.2	N/A	N/A
28	17	LV Mid inferolateral (EPI)			✓	17.3	✓	✓
29	18	LV Mid anterior		✓		19.1	✓	×
			n=11 (38%)	n=9 (31%)	n=9 (31%)	22.6 (14-36)	n=15 (83%)	n=7 (39%)

Figures

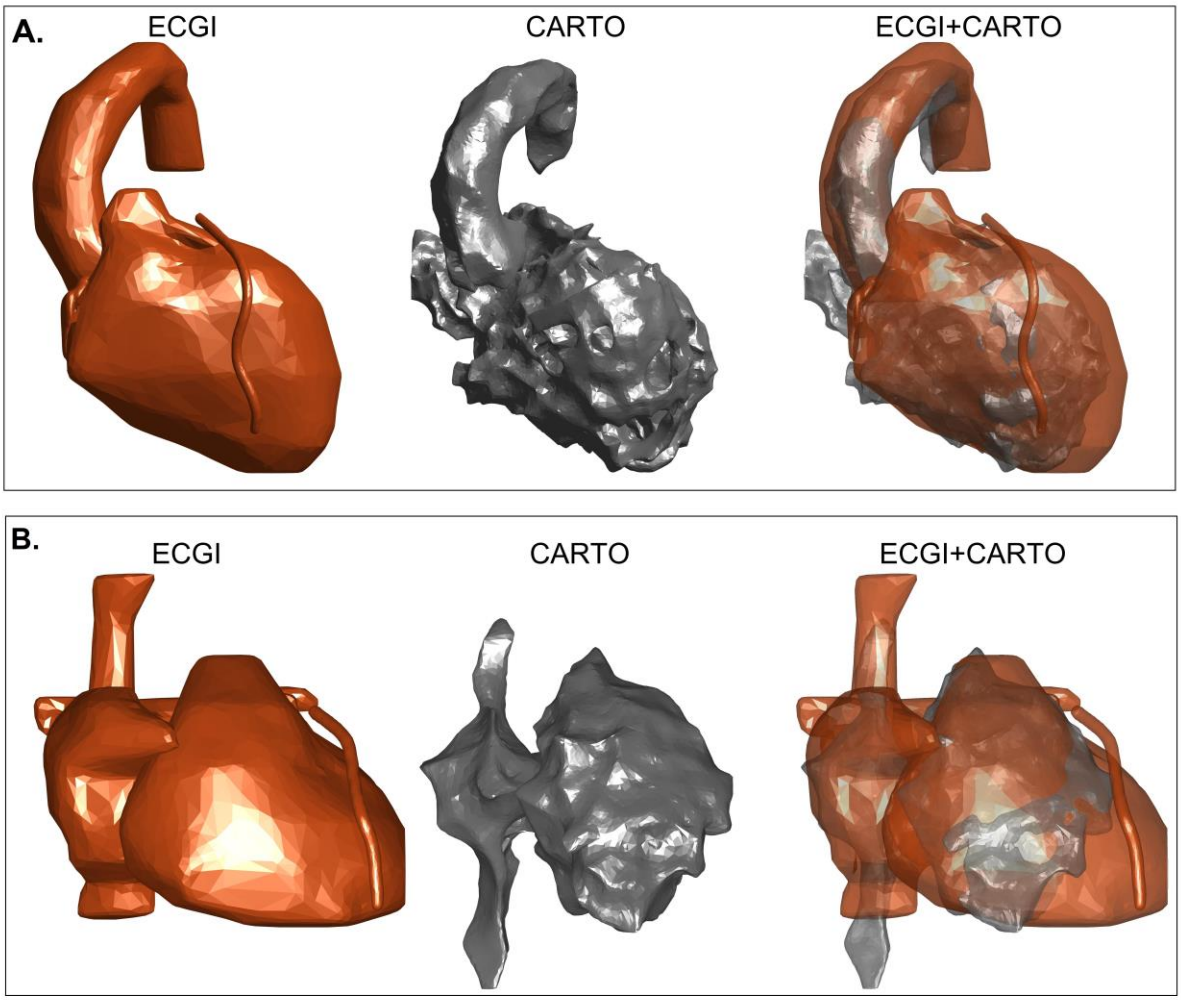

Figure 1: Anatomical co-registration of ECGI (left) and CARTO (middle) geometries in two patients. The two geometries are combined in the panel on the right. A – demonstrates the use of the Aorta for co-registration and in B the RVOT, IVC and SVC.

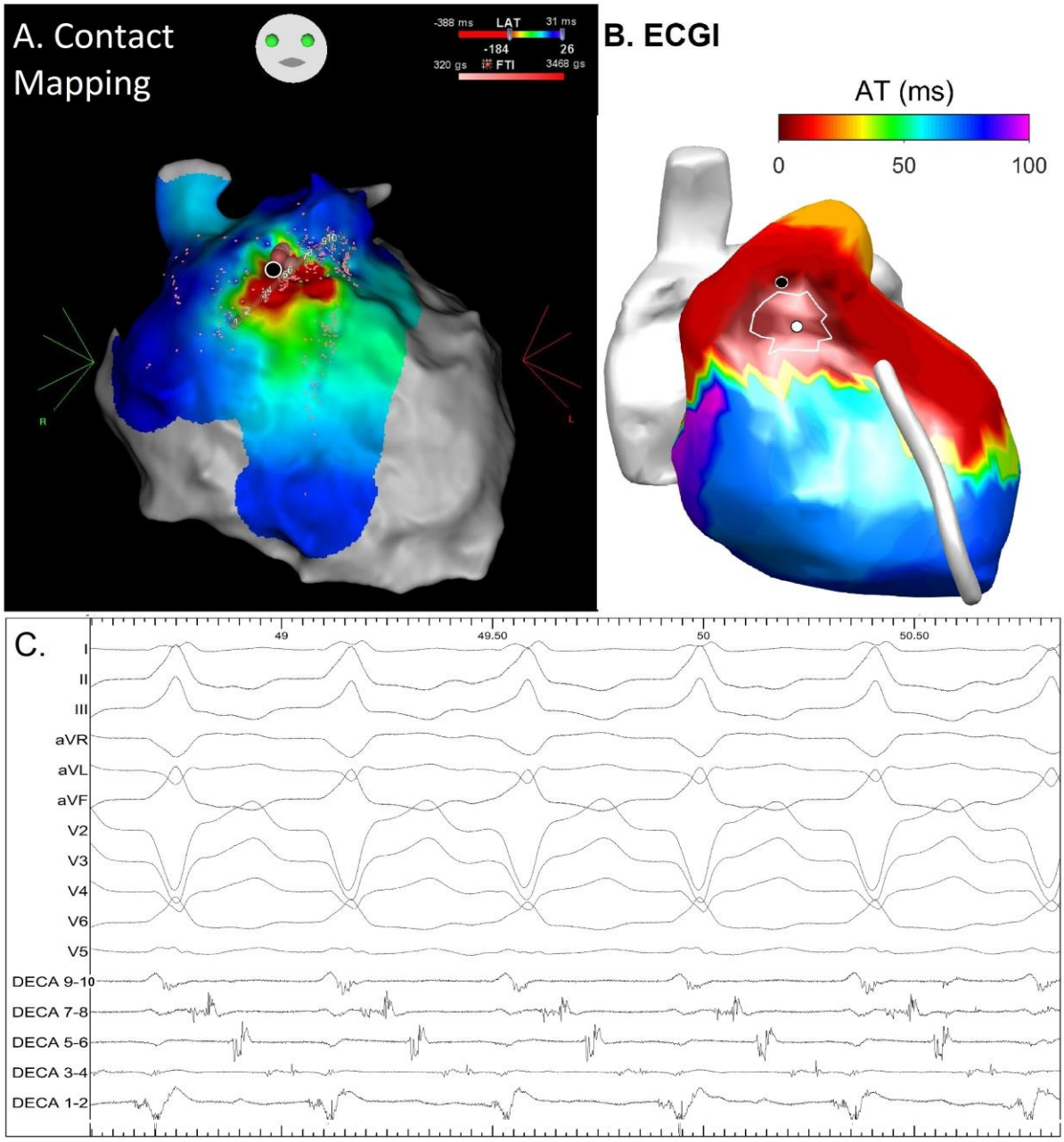

Figure 2: *Example from a VT terminated with ablation. A: Contact Electro-anatomical map (EAM) of a VT (patient #8, VT #13) shown in anteroposterior (AP) view. The red coloured area denotes diastolic activity seen on a Decapolar catheter overlying this area, with bipolar electrograms (EGMS) from this shown in panel C. Ablation tags (shown as red spheres) can be seen above the decapolar catheter, with the black circle highlighting the point from where VT was terminated during ablation. B: ECGI activation time (AT) map, shown in AP view, of the same VT. The area of earliest*

activation (lowest 2% of AT) is bordered by a white line and a white circle highlights its geometrical centre, which is the earliest site of activation. A black circle represents the nearest ECGI site to the VT site of origin (SoO) registered on the contact EAM. C: Surface ECG and intracardiac bipolar EGMs taken from decapolar catheter position as seen in panel A. Entrance to the isthmus can be seen on decapoles 7-8 with electrogram timing progressively later during the diastolic period until probable exit site in 1-2.

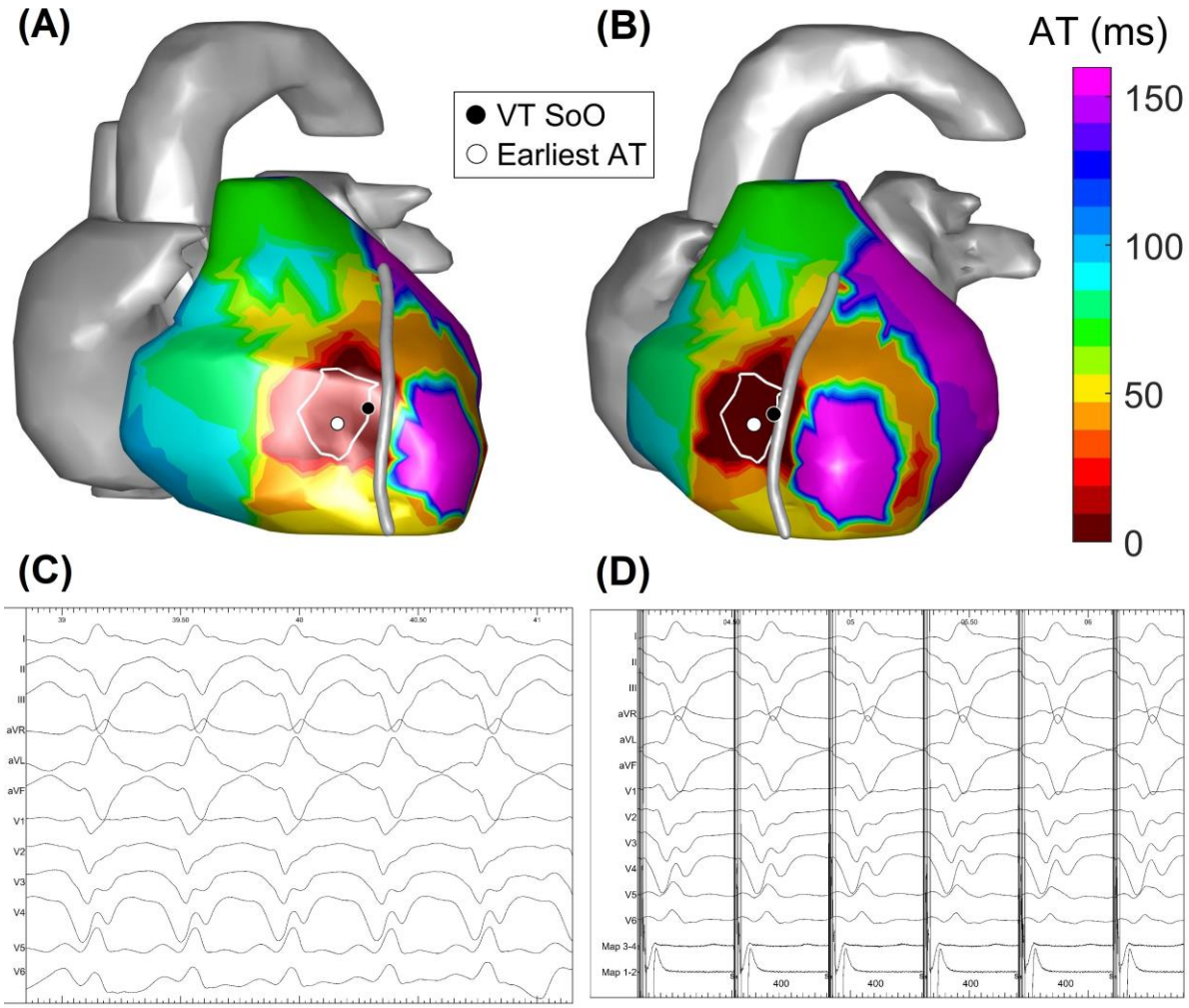

Figure 3: Example from a pace-mapped VT (patient #14, VT #24). Top: ECGI activation time map during VT shown in right and left anterior oblique views in A and B, respectively, with atria, IVC, SVC and aorta in grey. The region of earliest activation is bordered by a white line (lowest 2% of AT) and a white circle highlights its geometrical centre, which is the earliest site of activation. A black circle represents the nearest ECGI site to the VT site of origin (SoO) registered on the contact EAM and identified using pace-mapping. C: Surface ECG of the VT. D: Surface ECG during pace mapping of the VT. Paced rhythm had a 93% morphology match to the tachycardia (Template Matching, Bard EP system, Boston Scientific, MA, USA).

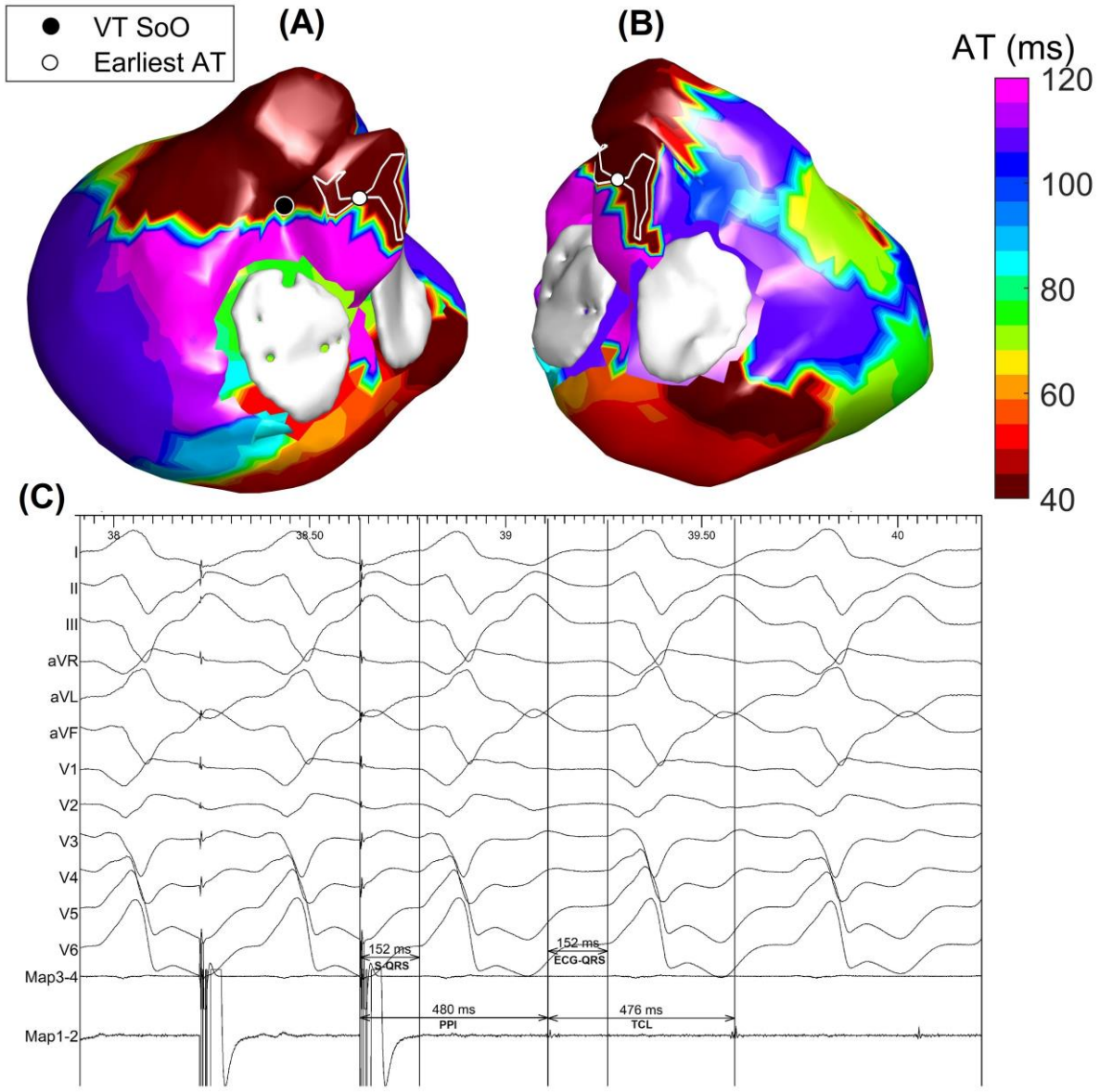

Figure 4: Example of an entrained VT (patient #11, VT #21). A: ECGI activation map during VT shown in standard PA view (panel A) and a modified PA view (panel B). The region of earliest activation is bordered by a white line (lowest 2% of AT) and a white circle highlights its geometrical centre, which is the earliest site of activation. A black circle represents the nearest ECGI site to the VT site of origin (SoO) registered on the EAM and identified using entrainment mapping. Activation occurs almost simultaneously on the LV basal anterior wall and RV basal inferior wall. Furthermore, the axis on the 12 lead ECG would suggest activation occurring from inferior to superior LV. This could be due to propagation of the re-entrant circuit exiting inferiorly

from the isthmus location on the basal antero-septum. A superior line of block would limit superior to inferior activation on the 12 lead ECG.C: Intracardiac electrograms demonstrating entrainment of tachycardia with a post pacing interval (PPI) minus tachycardia cycle length (TCL) of 4ms and identical timing for stimulus to QRS (S-QRS), and local electrogram to QRS (EGM-QRS).